Available online at www.sciencedirect.com
SCIENCE DIRECT®
International Journal of Mass Spectrometry 233 (2004) 361–371
International Journal of Mass Spectrometry
www.elsevier.com/locate/ijms

Review

Surface collisions of small cluster ions at incident energies 10–10^2 eV

Zdenek Herman [a,b,*]

[a] *V. Čermák Laboratory, J. Heyrovský Institute of Physical Chemistry, Academy of Sciences of the Czech Republic, Dolejškova 3, CZ-182 23 Prague 8, Czech Republic*
[b] *Institut für Ionenphysik, Leopold Franzens Universität, Technikerstrasse 25, A-6020 Innsbruck, Austria*

Received 10 November 2003; accepted 14 January 2004

This paper is dedicated to Tilmann D. Märk on the occasion of his sixtieth birthday as an expression of my respect to his personality.

Abstract

A short review of the field of collisions of slow cluster ions with surfaces is presented. The main subject of the paper is a survey of results of a series of studies on slow cluster ion collisions with surfaces carried out in Innsbruck. In these studies the incident ions were fullerene multiply-charged ions and small cluster ions of polyatomic molecules (acetone and acetonitrile radical cations, protonated ethanol, clustered by 2–4 monomer molecules). For collisions of multiply-charged fullerene cations C_{60}^{z+} (z from 1 to 5, incident energies 100–500 eV) only singly-charged product ions were observed which were formed by sequential loss of C_2 units. The effect of multiple-charge of the projectile on its fragmentation was less pronounced than expected from a full conversion of electronic energy gained in the surface neutralization process. Fragmentation upon surface collision excitation of acetone, acetonitrile and protonated ethanol cluster ions (incident energies 10–80 eV) was found to follow the unimolecular dissociation kinetics. Formation of protonated monomers in collisions of acetone and acetonitrile stoechiometric clusters resulted both from an intra-cluster reaction and from a reaction of the monomer product ion with the surface hydrogen; it could be rationalized using the double-well potential model. Incident energy dependence of relative abundance of dissociation products from surface collisions of protonated ethanol trimers, dimers and monomers could be mutually rationalized, if the fraction of energy transformed in the surface collision into internal energy was related to one internal degree of freedom. A diagram resembling a break-down pattern of the projectile ion was obtained in this way. All internal degrees of freedom of the projectile ion seemed to be involved in the unimolecular dissociation kinetics.

Keywords: Cluster ions; Surface collisions; Unimolecular dissociation; Chemical reactions at surfaces

1. Introduction

Studies of collisions of cluster ions with solid surfaces added another dimension to a wide range investigation of properties, reactivity and dynamics of cluster systems. The early interest was similar to the interest in studies of surface collisions of polyatomic molecular ions, namely in surface collision activation of projectiles to promote dissociative processes and possibly chemical reactions. However, very soon it turned out that collisions of cluster ions with surfaces exhibit an entire range of new phenomena connected with the specific features of these aggregate systems. This is reflected, for instance, in fragmentation phenomena of energized finite-size systems [1,2] in dependence on the energy deposited in them. Another specific feature is size-specific chemical reactivity of a cluster [3,4]. The subject of surface collisions of both clusters [5] and polyatomic ions [6] has been treated in excellent recent reviews. Theoretical studies of ion–surface and cluster–surface interactions employ a variety of methods. Molecular dynamics approaches or Monte Carlo simulation methods [7–9] have been used to describe various phenomena in gaseous particle–surface collisions over a wide range of energies from scattering to modification of materials and surface film formation [8,10]. Classical trajectory simulations with accurate potentials have been applied to study collisions of polyatomic ions [11] or protonated monomers, dimers, trimers, and pentamers of glycine [12–14] with surfaces.

Collisions of cluster ions with surfaces may lead to projectile dissociation (monomer evaporation and/or, in case of

* Tel.: +420-2-858-3014; fax: +420-2-858-2307.
E-mail address: zdenek.herman@jh-inst.cas.cz (Z. Herman).

1387-3806/$ – see front matter © 2004 Elsevier B.V. All rights reserved.
doi:10.1016/j.ijms.2004.01.011

molecular constituents, fragmentation of the constituents), to intra-cluster reactions, and to reactions of the projectile ion with the surface material. The character of fragmentation of a cluster upon surface-impact excitation depends on the incident energy. At low incident energies, clusters fragment by monomer evaporation. In the other extreme, high-energy surface collisions of cluster ions lead to prevailing disintegration of the projectiles. This "shattering" of the projectile was described to occur when the internal energy of the energized projectile exceeds a certain critical value and both theoretical [15–18] and experimental [18–21] evidence exists for its occurrence at larger impact energies. Fission of cluster ions into two fragments of about equal size was observed, together with evaporation, too. It was described for collisions of silicon anion clusters [22] and of certain metal anions and cations [23,24] at incident energies of tens of eV. Some alkali halide cluster ions were found to cleave to a series of two fragments of unequal size [25].

1.1. Dissociation via monomer evaporation

At low incident energies, if the energy transferred exceeds the binding energy of their constituents, cluster ions fragment by monomer evaporation. Monomer evaporation in ion cluster fragmentation, following deposition of low energies in them, has been usually described in terms of the evaporative ensemble model [2,26,27]. In surface collisions, the phenomenon was studied in detail in scattering of neutral atomic and molecular clusters and described in terms of the thermokinetic model [5,28]. This type of fragmentation is connected with a rather large mean lifetime of the energized species (order of hundreds of ps) and energy redistribution throughout the system before it starts to dissociate.

1.2. Shattering of cluster ions

Theoretical studies [29,30] of high energy collisions (keV range) of large atomic clusters indicated that in the system the effective temperature can reach thousands K and the effective pressure many GPa. These extreme conditions can lead to a novel type of fragmentation [15–18] and possibly induce novel chemical reactions in the system [31]. If the internal energy acquired in the surface collision is sufficiently high, the cluster shatters very quickly, in a time scale of a few picoseconds after excitation. This was shown to be due to fast energy equilibration within the system due to many-body intra-cluster collisions of the constituent particles. The phenomenon was demonstrated in theoretical and experimental [18] studies of surface impact of protonated ammonia ions, clustered by ammonia molecules, $NH_4^+(NH_3)_n$. The cluster ions did not decompose at all up to a critical incident energy of about 60 eV and then fragmented basically to monomers. From an analysis of product ion translational energy distribution it was concluded that this occurred within a timescale of less than 80 ps. A notable example is fragmentation of the fullerene ion C_{60}^+ [20] which starts to shatter at incident energies higher than about 300 eV to small even and odd numbered C_n^+ fragments of $n < 30$, while at lower energies it decomposes by sequential loss of C_2 units. The two fragmentation mechanisms overlap over a certain intermediate range of incident energies. Theoretical studies of dissociation of an iodine molecule embedded into a large argon cluster [32] indicated an efficient I–I bond breakup in a time scale shorter than its vibrational period. The impulsive process was attributed to a microscopic shock wave propagating through the cluster. Experimental support of the energy transport through the clustering molecules to the core ion that leads to its dissociation came from studies of dissociation of $N_3O_3^-(NO)_n$ (with n up to 40) [5]. Surface-induced fragmentation of protonated cluster cations $(H_2O)_nH^+$ ($4 \leq n \geq 32$) was found to be characterized by shattering of the projectile cluster ions to small molecular fragment ions, with notable absence of intermediate-size and large fragment ions [33].

1.3. Chemical reactions induced by surface collisions of cluster ions

A chemical reaction or a series of chemical reactions of a cluster ion can be induced by energy transferred in a surface collision. A recent study of collisions of $(CS_2)_n^-$ cluster ions with silicon and other surfaces [34] at incident energies above 100 eV may serve as an example to demonstrate the behavior of a system in which intra-cluster sequential reactions occur. Formation of different S_m^- fragments or their absence depended on the size of the incident cluster anion and could be connected with a series of intra-cluster reactions between the S^- fragment and constituent CS_2 molecules, analogous to elementary reactions in the gaseous phase.

Similarly as polyatomic molecular ions [6], cluster ions are know to react with the surface material. Pickup of C_2 units was observed in reactions of fullerene projectile ions with hydrocarbon-covered HOPG surfaces [20]. Addition of up to five C_2 units could be detected. H-atom transfer reaction and formation of a protonated product is a frequent process in collisions of open-shell molecular ions with hydrocarbon-covered surfaces [6]. An analogous process was observed in collisions of stoechiometric acetone [35,36] and acetonitrile [37] cluster ions with hydrocarbon-covered surfaces. The reactions and their competition with an intra-cluster surface-induced protonation reaction will be discussed later on in Section 3.2. Observation of the dication $(Na_nF_{n-2})^{2+}$ in collisions of alkali fluoride cluster ions $Na_nF_{n-1}^+$ with a clean silicon surface [38] was interpreted as a transfer of an F^- anion to the silicon surface. It may serve as an example of a process in which a particle is transferred from the projectile to the surface.

Surface collisions of clusters were suggested to drive chemical reactions with high energy barriers which do not occur easily. Theoretical calculations [32] predicted that, e.g., the four center reaction between N_2 and O_2 could

proceed to form NO, if the molecules were embedded into large clusters of noble gas atoms and the energy was supplied by an energetic surface collision. This suggestion was supported by subsequent experiments [39] in which $(CH_3I)_n^-$, $(CHF_3)_n^-$, and $(CHClF_2)_n^-$ cluster anions collided with diamond surfaces and formation of I_2^-, F_2^-, and ClF^-, respectively, was observed with a reaction probability increasing with cluster size as predicted by theoretical calculations.

1.4. Electron transfer in surface collisions of cluster ions

Electron transfer and neutralization of projectile cluster ions is an important process in surface collisions, similarly as in collisions of simple atomic and molecular ions with surfaces [6]. In the latter case, the electron exchange is influenced by the ionization potential (or recombination energy) of the projectile ion and by the work function of the surface. In cluster ions, an additional barrier to electron exchange represents the cluster envelope of the core ion. An quantitative study of this effect concerns collisions of $I_2^-(CO_2)_n$ with silicon surfaces [40] in which the probability of electron exchange, η_{ct}, was determined from experiments and also calculated as a tunneling process between the anion and the surface. Expressed as ion survival probability $S_A(\%) = 100(1 - \eta_{ct})$, the survival probability of the clustered iodine anions was of the order of several percent, larger than for "naked" I_2^- (close to 1%), and it increased with cluster size. Similarly, the total fragment-ion survival in collisions of protonated water ions $(H_2O)_nH^+$ ($4 \leq n \geq 32$) with a diamond surface was found to increase with the cluster ion size suggesting that the proton is solvated within the cluster [33].

Secondary electron emission connected with surface collisions of cluster ions concerns collisions at rather high incident energies (keV) and will not be discussed here.

1.5. Scope of the present review

This contribution is a short overview of the results obtained in studies of surface collisions of several small polyatomic cluster ions at incident energies up to about 100 eV (in studies of fullerene ions up to 500 eV), carried out in Innsbruck during the past 5 years. This energy regime may be viewed as an intermediate energy range between the low-energy monomer evaporation regime and high-energy regime of projectile shattering. In this regime cluster ion projectiles fragment not only by dissociation of monomers, but fragmentation of the constituent molecules takes place, too. This may lead to formation of clustered and/or non-clustered fragment ions of the constituent molecules. Also, intra-cluster chemical reactions and reactions of the cluster ion, induced by the surface collision could be observed. The systems investigated were clustered acetone molecular ions (up to tetramer) [35,36], clustered acetonitrile molecular ions (up to trimer) [37], and protonated ethanol cluster ions (up to trimer) [41]. From the measurements of mass spectra, one could make conclusions about the unimolecular character of dissociation of the projectile ions in dependence on the incident energy up to about 80 eV. Competition between the decomposition of the cluster ion, excited in a surface collision, and intra-cluster reaction of H-atom transfer in the radical cluster ion as well as the cluster reaction with the surface hydrogen was described and a model suggested. In addition, the effect of multiple charge of the projectile fullerene cation on the extent of surface-induced fragmentation was studied [42].

2. Experimental

The experiments were carried out on the Innsbruck tandem mass spectrometer BESTOF [36,43]. This device combines a cluster source with electron impact ionization of neutral clusters, a double-focusing sector field mass spectrometer for efficient analysis of projectile ions of high mass, a decelerator and a surface collision arrangement, and a time-of-flight detection of the surface-scattered ions. The projectile ions are mass analyzed at 3 keV and the beam is then decelerated towards the surface to an energy ranging from a few eV up to about several hundreds of eV. The projectile ion beam has a low energy spread of about 0.2 eV. The ions hit the surface at 45° (with respect to the surface) and the scattering angle is fixed at 91° with respect to the original beam direction. The scattered product ions are subjected to a pulsed extraction and acceleration that initiates the time of flight analysis in a linear TOF mass spectrometer. Mass spectra of product ions originating from surface collisions are recorded on a double-stage multichannel plate. The surface used in the experiments described here was a polished stainless steel surface covered with background hydrocarbons.

3. Results and discussion

3.1. Surface collisions of multiply charged fullerene ions: the effect of projectile charge on the extent of surface-induced dissociation

Considerable attention has been paid to collisions of positively and negatively charged fullerene ions with surfaces. Collisions of C_{60}^- with silicon surfaces revealed a remarkable stability of the cluster ions towards dissociation at incident energies below about 170 eV [44]. Results of scattering studies of C_{60}^+ impact with velocity and angular analysis of product ions [45,46] pointed out correlation between the parallel and perpendicular components of the velocity of surface collision products and provided information on the extent of collisional heating of the projectile. They also supplied further evidence for a two step model of fullerene ion surface collisions [46]: the projectile ion is first neutralized in the interaction with the surface and then reionizes after the

surface interaction by thermal electron emission. Its fragmentation could be described by the RRK formalism [46]. Careful detailed studies of fragmentation of C_{60}^+ and other fullerene ions [20] in surface collisions at 150–1050 eV revealed at low incident energies a sequential C_2 loss mechanism. However, at high incident energies, above 350 eV, another mechanism was found to take place which led to fission of the projectile to fragments of both odd and even number of C_n^+ atoms of n smaller than about 30. The sequential C_2 loss could be described by the RRKM unimolecular fragmentation mechanism [20,47]. The fit of experimental and calculated data led to an estimate of the average internal energy of the surface-excited projectile ions on different surfaces. On a HOPG surface covered by hydrocarbons the efficiency of collisional-to-internal energy transfer was estimated as $8 \pm 2\%$ and on a neat HOPG surface (cleaned by heating) it was about 15%. Initial internal energy of the projectile ions contributed to the extent of fragmentation.

In a series of experiments in Innsbruck, the extent of fragmentation of the fullerene ion in dependence on charge and incident energy was investigated [42]. Dissociative and reactive processes upon interaction of singly- and multiply-charged fullerene ions C_{60}^{z+} ($z = 1$–5) of energies 100–500 eV in collisions with a stainless steel surface covered by hydrocarbons were studied. For singly-charged fullerene ions, the results were in general agreement with the above mentioned results of ref. [20]. In collisions of multiply-charged fullerene ions, only singly-charged product ions were observed. An example of the spectra at 400 eV for ion projectiles C_{60}^{5+} and C_{60}^{4+} is shown in Fig. 1. The fragmentation occurs by dissociation of C_2 fragments. The extent of fragmentation increased with the incident energy for the fullerene ions of the same charge (Fig. 2, right). Similarly, the extent of fragmentation increased, at the same incident energy, with the charge of the projectile ion (Fig. 2, left). However, the effect of charge was smaller than expected from a full conversion of the energy gained by the partial neutralization process to internal energy available for fragmentation of the singly-charged ion. This energy ranges from about 6 eV for $z = 2$ to about 55 eV for $z = 5$ [42].

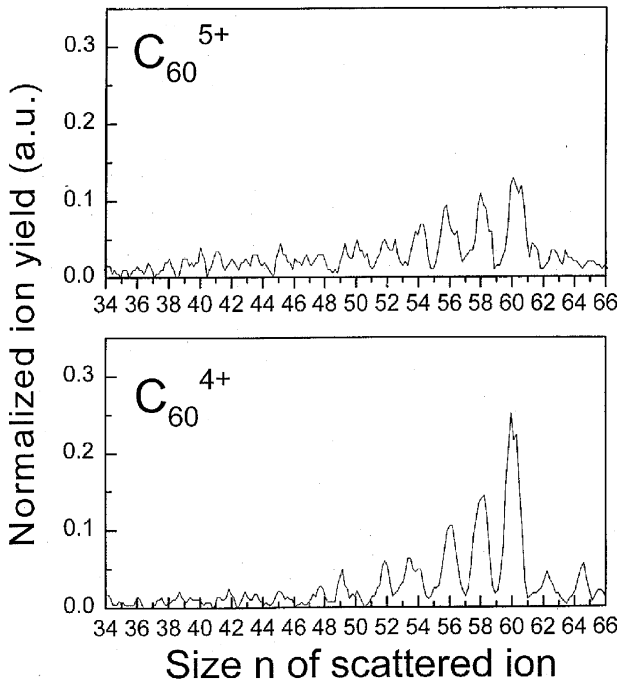

Fig. 1. Mass spectra of C_n^+ products of surface collision dissociation of C_{60}^{5+} and C_{60}^{4+} at the incident energy of 400 eV [42].

To quantify the effect of the increasing charge and the increasing incident energy of the fullerene projectile fragmentation, average internal energy E'_{int} of the scattered C_{60}^+ was estimated from the extent of fragmentation. The calculations assumed the generally accepted model of fullerene ion surface interaction: the incident ion is first neutralized and vibrationally excited in the surface collision; thereafter

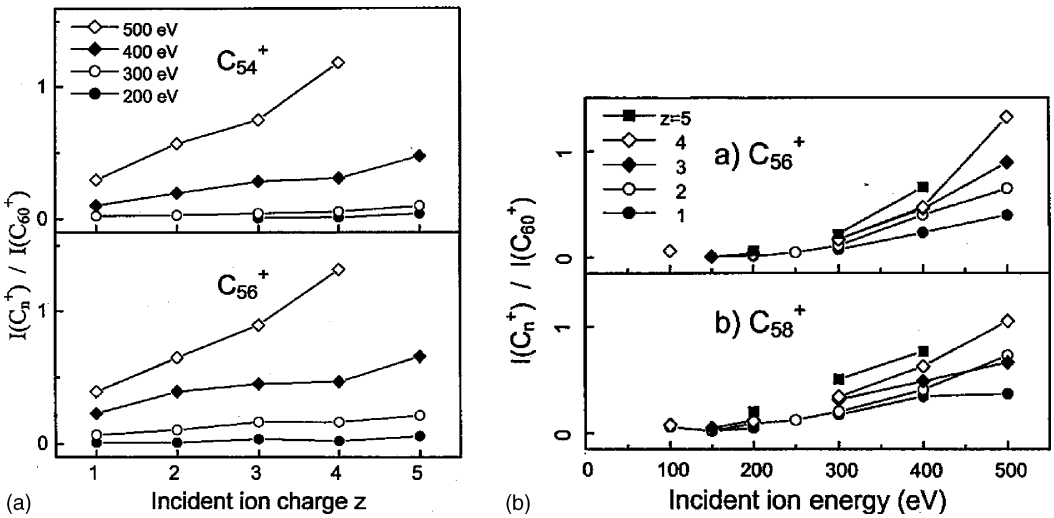

Fig. 2. Relative abundance $I(C_n^+)/I(C_{60}^+)$ of product ion from surface collisions of C_{60}^{n+} in dependence on incident ion charge (left) and incident energy (right) (adapted from data in ref. [42]).

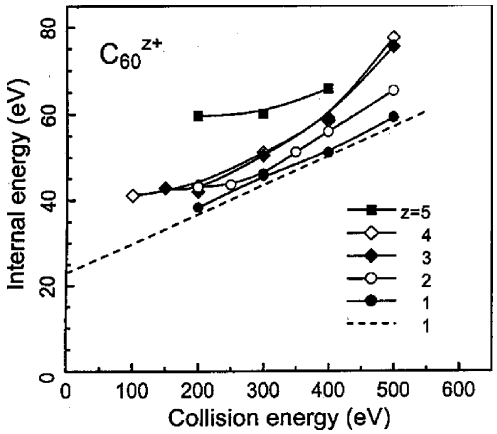

Fig. 3. Average internal energy of surface-excited ions C_{60}^{+} from collisions of C_{60}^{z+} ($z = 1$–5) in dependence on the incident projectile energy as estimated from product ion distribution. The dashed line represents data for $z = 1$ from ref. [20].

it rapidly autoionizes by thermally-activated electron emission and fragments by sequential loss of C_2 units. An Arrhenius expression was used to determine the rate constant of dissociation and the vibrational temperature of the ion. The distribution of internal energies in the excited scattered projectile was assumed to be Gaussian, with the peak value and the width variable to achieve the best fit between simulated fragment distribution and experimental spectra.

The resulting dependence of the average internal energy of the scattered C_{60}^{+} on incident projectile energy, with the projectile charge as a parameter is shown in Fig. 3. For $z = 1$ the average internal energy increases practically linearly with the incident energy, in good agreement with data of ref. [20] (dashed line). The slope leads to the value of translational-to-internal energy transfer of $6.8 \pm 0.5\%$. For higher charges of the fullerene projectiles, $z > 1$, the average internal energy content is somewhat higher, but the dependence on incident energy is not linear and somewhat irregular. At incident energies higher than about 300 eV the increase with charge is about 20–30% of the energy expected to be gained by neutralization. This suggests that the surface may act as an energy sink during the surface collision of the neutralized projectile.

3.2. Surface collisions of acetone and acetonitrile cluster ions: intra-cluster reaction and surface reaction of clustered radical cation

Stoechiometric deuterated acetone cluster ions $(CD_3COCD_3)_n^{\bullet+}$ ($n = 2$–4) were prepared by electron impact ionization of a neutral acetone cluster beam. The open-shell molecular ions, clustered by acetone molecules, formed the main progression in the electron impact mass spectrum (besides protonated dimer ions and clustered CD_3CO^+ fragment ions) [36]. Selected dimer, trimer and tetramer ions collided with the surface with defined energies (6–80 eV) and the product ions were recorded. Activation by energy transfer in the surface collision led to fragmentation of the cluster ions. The main dissociation products were the monomer ion $(CD_3COCD_3)^{\bullet+}$, protonated and deuteronated (i.e., with attached D^+ instead of H^+) monomer, $(CD_3COCD_3)H^+$ and $(CD_3COCD_3)D^+$, and dissociation products of these ions, CD_3CO^+, CD_2OD^+, CD_2OH^+, and at higher incident energies CD_3^+. Fig. 4 shows, as an example, recorded mass spectra obtained by impact of deuterated acetone dimer and tetramer ions, $(CD_3COCD_3)_2^{\bullet+}$ and $(CD_3COCD_3)_4^{\bullet+}$ at several incident energies. Of the cluster ions, only small amounts of the dimer $(CD_3COCD_3)_2^{\bullet+}$, were observed in trimer ion collisions at incident energies below 20 eV.

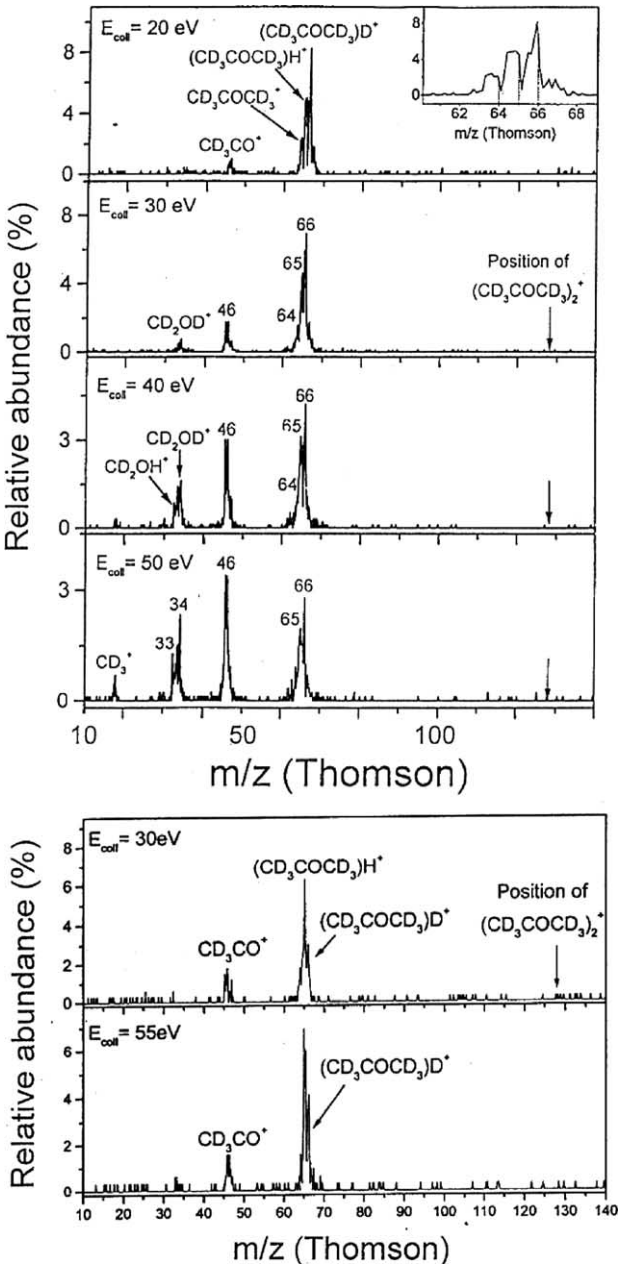

Fig. 4. Mass spectra of product ions from collisions of acetone dimer $(CD_3COCD_3)_2^{\bullet+}$ (upper part) and acetone tetramer $(CD_3COCD_3)_4^{\bullet+}$ (lower part) at several incident energies (adapted from ref. [36]).

The protonated and deuteronated product ions originate in chemical reactions of the projectile ion, activated by the surface collision. The deuteronated ion $(CD_3COCD_3)D^+$ results from an intra-cluster reaction (formulated for collisions of a dimer ion):

$$(CD_3COCD_3)_2{}^{\bullet+} + S/RH \rightarrow (CD_3COCD_3)_2{}^{\bullet+*} \rightarrow (CD_3COCD_3)D^+ + CD_2COCD_3{}^{\bullet} \quad (1)$$

and the protonated acetone ion $(CD_3COCD_3)H^+$ by H-atom transfer reaction between the projectile and the surface hydrogen:

$$(CD_3COCD_3)_2{}^{\bullet+} + S/RH \rightarrow (CD_3COCD_3)H^+ + CD_3COCD_3 + S/R^{\bullet} \quad (2)$$

Mutual competition of the two processes can be rationalized by adopting the principle of Brauman's double-well model of ion–molecule reactions [48]. Fig. 5 illustrates the model for the simplest case of dimer collisions. The acetone dimer ion, relaxed by monomer evaporation from larger acetone cluster ions to low internal energies, exists before the interaction with the surface in two different configurations, $(CD_3COCD_3)D^+ \cdot (CD_2COCD_3)^{\bullet}$ and $(CD_3COCD_3) \cdot (CD_3COCD_3)^{\bullet+}$, separated by a barrier. The minima represent schematically the energetics of shifting the position of the bridging deuterium in the dimer. The

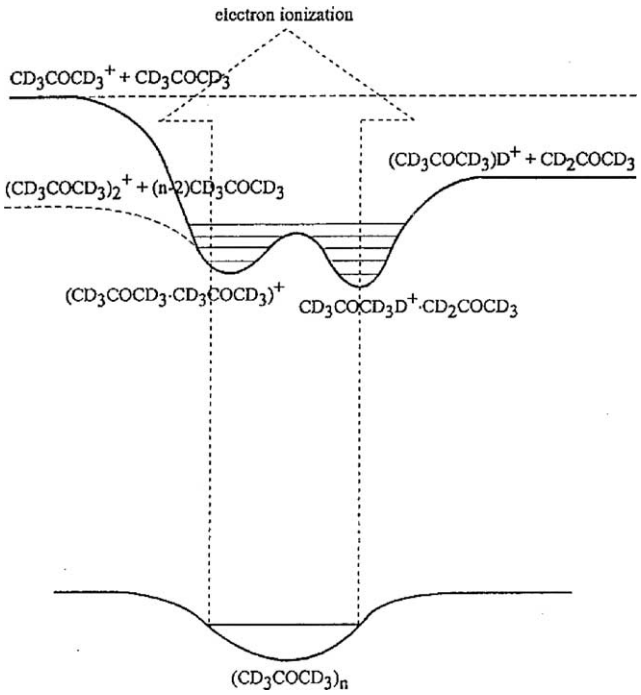

Fig. 5. Schematic view of the Brauman double-well potential for the acetone dimer ion. Model representation of dissociation of the surface-excited dimer cation into either $(CD_3COCD_3)D^+ + CD_2COCD_3{}^{\bullet}$ (intra-cluster reaction) or $CD_3COCD_3{}^{\bullet+} + CD_3COCD_3$ (the molecular radical cation partly reacts further with surface hydrogen to $(CD_3COCD_3)H^+$).

binding energy of the dimer ion can be roughly estimated to about 1 eV. Also, from the relatively strong hydrogen bonds in acetone neutral clusters one could estimate that evaporation of an acetone molecule from the cluster removes about 0.3 eV. Successive monomer evaporation relaxes the incoming cluster ion to low internal energy levels in the Brauman potential wells. The internal energy of the intermediate prior to surface impact may be estimated as <0.3 eV. In the surface collision a small fraction of projectile translational energy (about 6% of the incident energy for surfaces covered by hydrocarbons) is converted into the internal energy of the dimer ion and this leads to dissociation of the two moieties to ions $(CD_3COCD_3)D^+$ and $(CD_3COCD_3)^{\bullet+}$, depending on the configuration of the system in the moment of surface interaction. In the latter case, most of the open-shell molecular acetone ions may react with the surface hydrocarbons to give by hydrogen abstraction the protonated acetone as a major product. Molecular radical cations $(CD_3COCD_3)^{\bullet+}$ were also observed as a less abundant reaction product. Some of these may be ions which—after dissociation at the surface—could not react to $(CD_3COCD_3)H^+$, some may have been formed in slow unimolecular dissociations of the receding dimer ion to $(CD_3COCD_3)^{\bullet+} + (CD_3COCD_3)$, after the interaction with the surface.

An analogous case represent surface collisions of stoechiometric acetonitrile cluster ions (dimers and trimers). Fig. 6 shows the relative abundance of product ions in dependence on the incident energy for several projectile ions (collision energy resolved mass spectra, CERMS curves). The incident ions were acetonitrile dimer ions, $(CH_3CN)_2{}^{\bullet+}$ (Fig. 6a), deuterated acetonitrile dimer ions, $(CD_3CN)_2{}^{\bullet+}$ (Fig. 6b), and deuterated acetonitrile trimer ions, $(CD_3CN)_3{}^{\bullet+}$ (Fig. 6c). The data in Fig. 6 indicate, for the dimer projectiles, considerable amounts of non-dissociated dimer ions up to incident energies of 25 eV, and partial dissociation to monomer above about 5 eV. The main process at higher incident energies, however, is a surface collision-induced chemical reaction to form protonated acetonitrile. In collisions of $(CH_3CN)_2{}^{\bullet+}$ this product is CH_3CNH^+. Collisions of $(CD_3CN)_2{}^{\bullet+}$ reveal that both CD_3CND^+ and CD_3CNH^+ ions were formed. The former is evidently a product of intra-cluster reaction, analogous to reaction (1) in surface collisions of acetone cluster ions. The latter product, CD_3CNH^+, results from a reaction with surface hydrogen, analogous to reaction (2). The products at 10 eV show the non-dissociated trimer and partial dissociation to the dimer ion and a monomer molecule. At a slightly higher energy (15 eV) the main dissociation product is the dimer and its reaction products: the energized dimer gives in an intra-molecular reaction, analogous to (1), deuteronated acetonitrile CD_3CND^+ and the reactive molecular radical cation $CD_3CN^{\bullet+}$ which mostly reacts with the surface hydrogen to form CD_3CNH^+. The sum of the curves CD_3CNH^+ and CD_3CND^+ in Fig. 6b adds rather well to fit the curve for CD_3CNH^+ in Fig. 6a. An analogous double-well model as described above (Fig. 5) can be

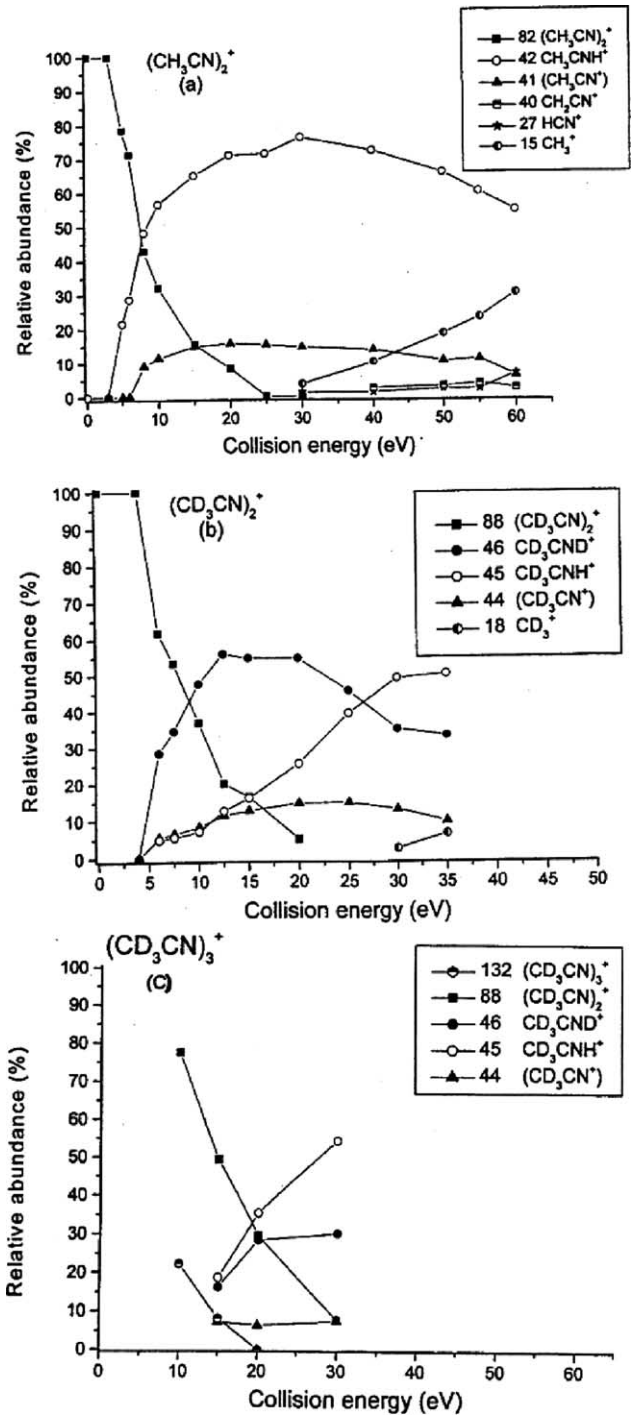

Fig. 6. CERMS curves of product ions from surface interactions of acetonitrile cluster ions. Projectile ions (a) $(CH_3CN)_2^{\bullet+}$; (b) $(CD_3CN)_2^{\bullet+}$; (c) $(CD_3CN)_3^{\bullet+}$ (adapted from ref. [37]).

used to explain the occurrence of both the intra-molecular deuteron transfer reaction in the energized cluster ion and the H-atom reaction with the surface hydrogen.

The CERMS curves for the trimer projectile ion, $(CD_3CN)_3^{\bullet+}$ in Fig. 6c show the presence of non-dissociated trimer ions up to about 20 eV and the occurrence of the dimer $(CD_3CN)_2^{\bullet+}$ (formed evidently from the trimer by dissociation of one monomer molecule) up to energies of about 30 eV, besides $CD_3CN^{\bullet+}$ and the reaction products CD_3CND^+ and CD_3CNH^+. The presence of the trimer and dimer in the dissociation products indicates that unimolecular dissociation kinetics governs the product ion formation in surface collisions of these cluster systems at incident energies up to about 30 eV.

3.3. Surface collisions of protonated ethanol cluster ions: unimolecular dissociation and the protonated trimer break-down graph

Surface-induced dissociation of protonated ethanol cluster ions $(C_2H_5OH)_nH^+$ ($n = 1$–3) was investigated in the incident energy range of 10–80 eV to elucidate the mechanism of dissociation of small closed shell cluster ions that do not chemically react with the surface [41]. The formation of protonated alcohol cluster ions upon electron impact ionization of neutral ethanol clusters was ascribed earlier [49] to the reaction:

$$\begin{aligned}&(\text{R-CH}_2\text{OH})_n + e^- \\ &\rightarrow (\text{R-CH}_2\text{OH})_{n-m-1}\text{H}^+ \\ &\quad +(\text{R-CH}_2\text{OH})_m \cdot \text{R-CH}_2\text{O}^\bullet + 2e^- \end{aligned} \quad (3)$$

Dissociation processes of alcohol cluster ions upon electron impact were investigated as well as their gas phase reactivity. In SIFT experiments at thermal energies [50] ligand switching, proton transfer, solvent evaporation, and association reactions were observed. Activation energies for decomposition of proton-bound dimers were estimated from thermochemical data and for ethanol dimer decomposition to ethanol molecule and protonated ethanol the value of 32 kcal/mol (1.4 eV) was derived [51].

The electron impact mass spectrum of neutral ethanol cluster beam contained only protonated cluster ions, the stoechiometric ions were absent in the spectrum [41]. The main process observed after the surface collision activation was dissociation. No chemical reactions of the protonated cluster ions with the surface material were observed. Recorded mass spectra of product ions upon surface impact of protonated monomers showed fragmentation of $(C_2H_5OH)H^+$ to products H_3O^+ and $C_2H_5^+$ with subsequent dissociation to $C_2H_3^+$, i.e., typical processes of closed-shell protonated ion dissociations with a loss of a neutral molecule. The CERMS curves of the surface-induced dissociation of the protonated ethanol monomer are shown in Fig. 7c. Mass spectra of product ions obtained from surface-induced processes upon impact of protonated dimer ions (Fig. 7b) indicated the presence of the protonated monomer ion, formed up to incident energies of about 50 eV, and its fragmentation products H_3O^+, $C_2H_5^+$, and $C_2H_3^+$. Mass spectra of product ions upon the trimer projectile impact (Fig. 7a) showed fragmentation of the protonated trimer to protonated dimer, protonated monomer, and fragment ions of the protonated monomer. The CERMS curves for the pro-

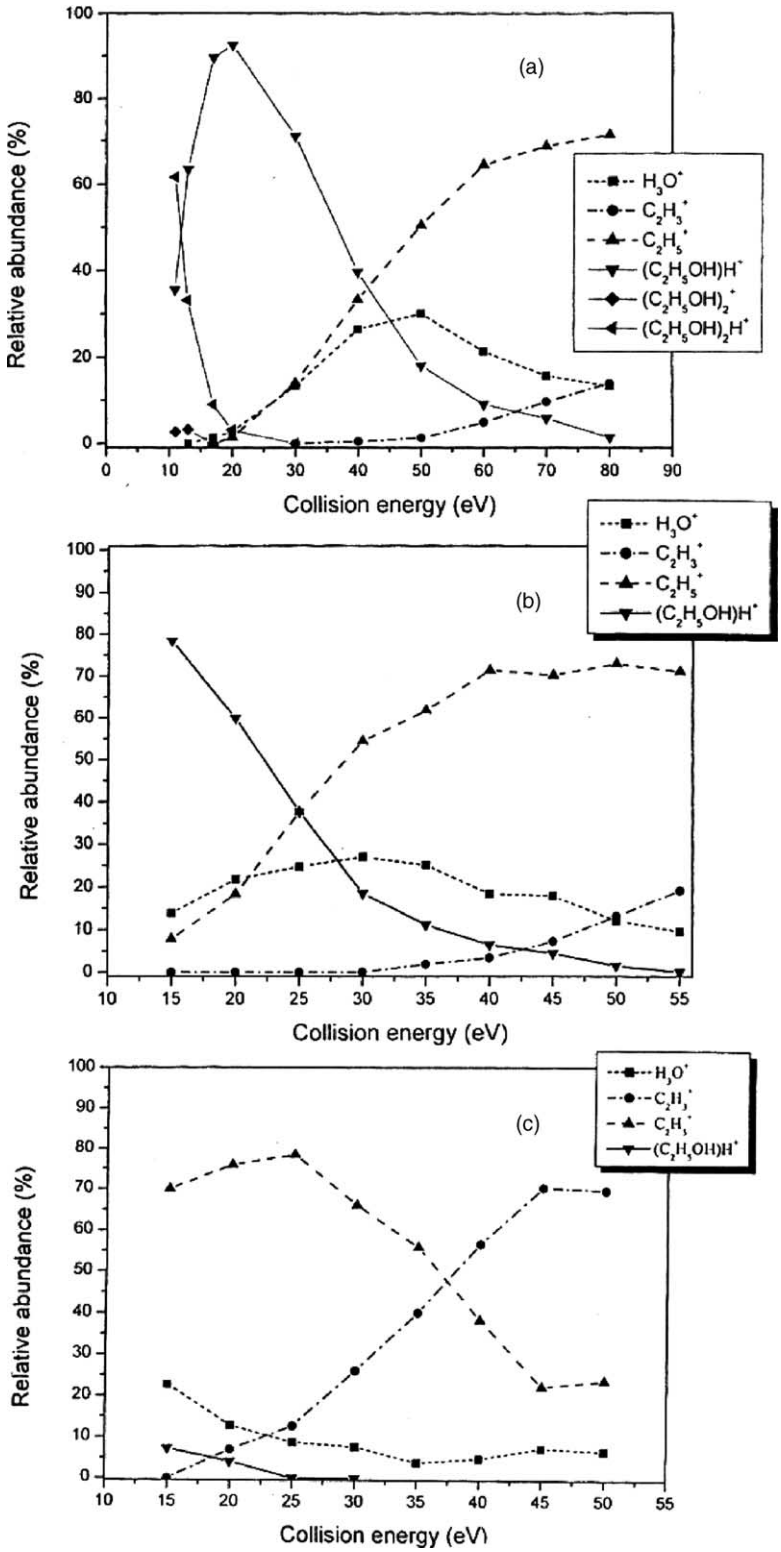

Fig. 7. CERMS curves of product ions from surface interactions of protonated ethanol cluster ions. (a) Protonated trimer $(C_2H_5OH)_3H^+$; (b) protonated dimer $(C_2H_5OH)_2H^+$; (c) protonated monomer$(C_2H_5OH)H^+$ (adapted from ref. [41]).

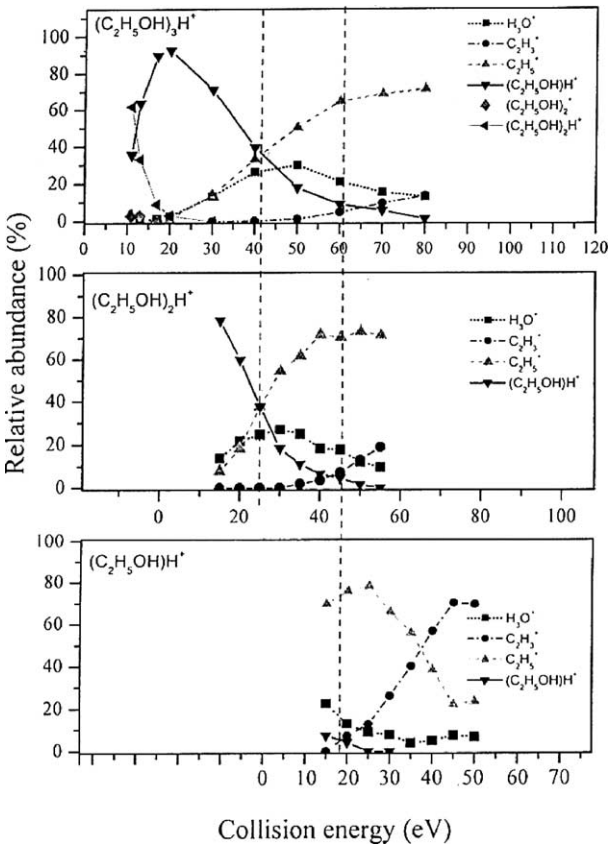

Fig. 8. CERMS curves from Fig. 7 with incident energy scale shifted to fit the characteristic crossing of particular ion abundance (see text and ref. [41]).

tonated ethanol trimer, dimer and monomer are given in Fig. 7. It can be seen from Fig. 7 that the CERMS curves for the three projectile cluster ions show similar features, namely crossings between different product ion abundance, occurring, however, at different incident energies. For instance, in the CERMS curves for protonated monomer and dimer impact, the characteristic crossing between the abundance of the product ions $(C_2H_5OH)H^+$ and $C_2H_5{}^+$, in the CERMS curves of all three projectiles, the crossing between abundance of $(C_2H_5OH)H^+$ and $C_2H_3{}^+$ and of H_3O^+ and $C_2H_3{}^+$.

By plotting the CERMS curves from Fig. 7 above each other and shifting the incident energy scale of the protonated dimer by 16 eV with respect to the protonated trimer curve, and the protonated monomer $(C_2H_5OH)H^+$ curves by 45 eV with respect to the timer curve, one can place the characteristic crossing above each other and see approximate similarities on the CERMS curves of the three projectiles (Fig. 8). However, the character of the similarities is only approximate: it appears that the incident energy scale is more and more compressed when going from the CERMS curves of the protonated trimer to the protonated monomer. The shifts in the abscissa of the incident energy scale for the particular projectile ions suggest that they may be related to the binding energies of the ethanol monomer molecules to the various projectile ions. If one assumes that the efficiency of the collision-to-internal energy transfer on the hydrocarbon-covered metal surface is about 6% (this value is based on surface-induced dissociation of such diverse projectile polyatomic ions like the fullerene ion [20,42] or the ethanol molecular ion [52,53]), one can derive from the shifts of the energy scale in Fig. 6 an approximate value for the dissociation energy of the ethanol molecule from the protonated ethanol trimer ion, $D[(C_2H_5OH)_2H^+ - (C_2H_5OH)] = (41 - 25)0.06 = 0.95$ eV, and for the protonated dimer $D[(C_2H_5OH)H^+ - (C_2H_5OH)] = (45 - 18)0.06 = 1.6$ eV. These values are in good agreement with the calculated binding energies [54] of ethanol molecules in protonated ethanol cluster ions of 0.92 eV for the trimer and 1.38 eV for the dimer, respectively, and the earlier published value [51] for the dimer, 1.39 eV. The agreement between these published binding energies and the values derived from this analysis in turn provides another independent support for the above adopted value of the translational-to-internal energy transfer efficiency of 6% of the incident energy on the type of surface used.

The above mentioned compression of the CERMS curve patterns when going from the protonated monomer to trimer projectile in Fig. 8 results from the fact that the energy available is distributed over different number of integral degrees of freedom. A simple unification of the picture was achieved by normalizing the energy scale to the energy pertinent to a single degree of freedom, $\langle E_{int}\rangle_{idf}$. Assuming that the system behaves as a statistical ensemble, this means dividing the abscissa energy scale by $(3N - 6)$ and accepting 6% as the factor of collisional-to internal energy transfer on this surface, $\langle E_{int}\rangle_{idf} = 0.06E_{coll}/(3N - 6)$. The CERMS curves from Figs. 7 and 8 are plotted in this way in Fig. 9. The fit of the mutually overlapping and extending data is quite satisfactory. One thus obtains a unimolecular decomposition pattern of the protonated trimer projectile over a wide range of energies by a combination of surface-dissociation data of three different projectiles. The internal energy of the trimer is then simply $\langle E_{int}\rangle_3 = (3N_3 - 6)\ \langle E_{int}\rangle_{idf} = 78\langle E_{int}\rangle_{idf}$ (upper scale in Fig. 9). The average width of the energy transferred in the surface collision, as derived from combination of available data (see references cited in [41]), is shown in the right part of Fig. 9.

The analysis of the results of surface-induced dissociation of protonated ethanol clusters showed: (i) surface-induced dissociation of the protonated clusters of this type follows the model of unimolecular dissociation of a cluster that can be regarded as a statistical ensemble. (ii) Mutual consistence of the data in Fig. 7 indicates that in this ensemble all internal degrees of freedom are involved. (iii) The translational-to-internal energy transfer in the surface collision with the hydrocarbon-covered stainless steel surface amounts to about 6% of the incident energy, the internal energy transferred increases linearly with the incident energy, and the width of the energy distribution does not change appreciably with the incident energy. Thus, the CERMS curves

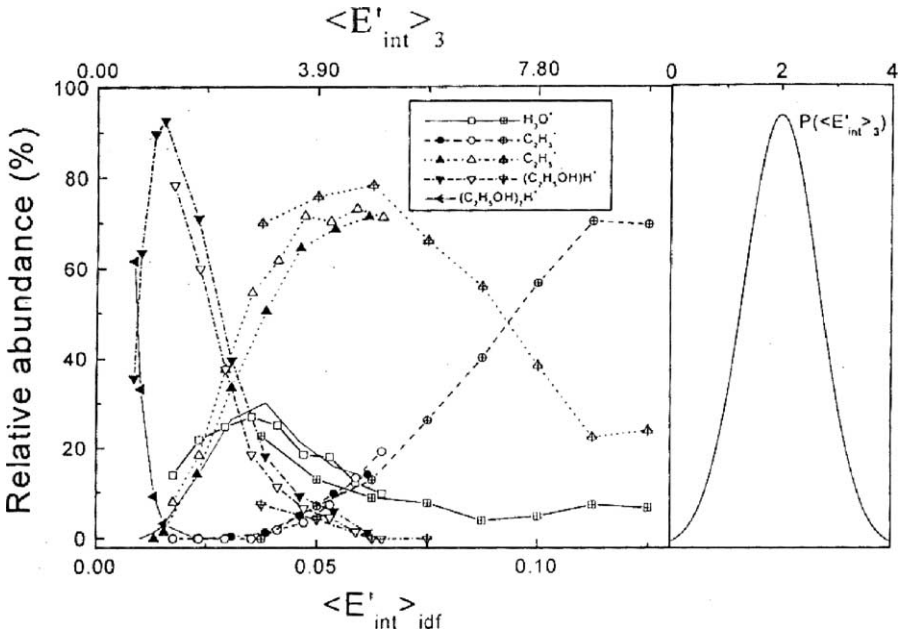

Fig. 9. Breakdown pattern of the protonated ethanol trimer $((C_2H_5)OH)_3H^+$ as obtained from CERMS curves of product ions from surface collisions of the protonated ethanol monomer, dimer and trimer. Dependencies of relative abundance of fragment ions on internal energy of the surface-excited projectile pertinent to one internal degree of freedom $\langle E'_{int}\rangle_{idf}$. Data from Figs. 6 and 7. Upper scale shows the recalculated internal energy of the protonated trimer. The curve on the right side represents a typical internal energy distribution transferred in a surface collision of a polyatomic ion on a metal surface covered with hydrocarbons (details see ref. [41]). Both upper ($\langle E'_{int}\rangle_3$) and lower ($\langle E'_{int}\rangle_{idf}$) abscissa scale in eV.

provide a good basis for the determination of the unimolecular fragmentation pattern (analogous to break-down patterns of polyatomic molecular ions) of polyatomic protonated cluster projectiles, i.e., species for which no neutral precursor exists. This finding for cluster ions supports the earlier suggestion of Cooks and coworkers [55] that surface collision can be used to impart a well-defined energy to a polyatomic projectile ion and that CERMS curves reflect the unimolecular break-down pattern of the projectile ion.

4. Conclusions

The studies described above bring information on the kinetics of dissociation of simple cluster ions, formed by polyatomic monomers, at incident energies 10–80 eV. The results indicate that in this energy regime, the fragmentation can be described in terms of the unimolecular dissociation model. An important result is involvement of all integral degrees of freedom in the fragmentation of protonated ethanol trimers, dimers and monomers. The possibility to obtain break-down patterns for polyatomic systems for which there exists no stable molecular precursor from surface collision data is of interest, too, though the data may be smeared out due to rather broad range of energies transferred into internal energy of the projectile in the surface excitation process. Relevant RRKM calculations, currently under way, will show how much this possibility can be exploited. Formation of protonated monomers in collisions of acetone and acetonitrile stoechiometric clusters was found to result both from an intra-cluster chemical reaction and from an H-atom transfer reaction of the monomer product ion with the surface hydrogen and it could be rationalized using the double-well potential model. In collisions of multiply-charged fullerene ions, unimolecular dissociation, characterized by sequential C_2 fragment loss, seems to govern the fragmentation at collision energies up to several hundreds eV. The influence of the internal energy gained from multiply-charged projectile neutralization is less than expected from the nominal energy difference.

Acknowledgements

I wish to thank to all collaborators in the research described here. I am indebted to H. Yasumatsu and T. Kondow for providing access to their recent work. Partial support of the grants Kontakt 2000-01, No. 6 and Kontakt ME 561 (Ministry of Education, Youth and Sports, Czech Republic), Association EURATOM-IPP.CR, and European 5th Programme Network MCI (Generation, Structure and Reaction Dynamics of Multiply-Charged Ions) during preparation of this manuscript is gratefully acknowledged.

References

[1] D. Beyson, X. Campi, E. Pfefferkorn (Eds.), Fragmentation Phenomena, World Scientific, Singapore, 1995.

[2] C. Mair, J. Fedor, M. Lezius, P. Scheier, M. Probst, Z. Herman, T.D. Märk, New J. Phys. 5 (2003) 9.1.
[3] M.B. Knickelbein, Annu. Rev. Phys. Chem. 50 (1999) 79.
[4] M. Ichihashi, T. Hammura, R.T. Yadav, T. Kondow, J. Phys. Chem. A 104 (2000) 11885.
[5] H. Yasumatsu, T. Kondow, Reports Prog. Phys. 66 (2003) 1783.
[6] V. Grill, J. Shen, C. Evans, R.G. Cooks, Rev. Sci. Instrum. 72 (2001) 3149.
[7] B.J. Garrison, P.D.S. Kodali, D. Srivastava, Chem. Rev. 96 (1996) 1327.
[8] L. Hanley, S.B. Sinnott, Surf. Sci. 500 (2002) 500, and references therein.
[9] W. Eckstein, Computer Simulation of Ion–Solid Interactions, Springer, New York, 1991.
[10] Y. Hu, S.B. Sinnott, Surf. Sci. 526 (2003) 230.
[11] O. Meroueh, W.L. Hase, Phys. Chem. Chem. Phys. 3 (2001) 2306.
[12] O. Meroueh, W.L. Hase, J. Am. Chem. Soc. 124 (2002) 1524.
[13] O. Meroueh, Y. Wang, W.L. Hase, J. Phys. Chem. A 106 (2002) 9983.
[14] J. Wang, S.A. Meroueh, Y. Wang, W.L. Hase, Int. J. Mass Spectrom. 230 (2003) 57.
[15] E. Hendell, U. Even, T. Raz, R.D. Levine, Phys. Rev. Lett 75 (1995) 2670.
[16] T. Raz, U. Even, R.D. Levine, J. Chem. Phys. 103 (1995) 5394.
[17] U. Even, T. Kondow, R.D. Levine, T. Ray, Comments At. Mol. Phys. D 1 (1999) 1.
[18] W. Christen, U. Even, T. Raz, R.D. Levine, Int. J. Mass Spectrom. Ion. Process. 174 (1998) 35.
[19] P. Weiss, J. Rockenberg, R.D. Beck, M.M. Kappes, J. Chem. Phys. 104 (1996) 3629.
[20] R.D. Beck, J. Rockenberger, P. Weiss, M.M. Kappes, J. Chem. Phys. 104 (1996) 3638.
[21] R.D. Beck, C. Warth, K. May, M.M. Kappes, Chem. Phys. Lett. 257 (1996) 557.
[22] P.M.St. John, R.L. Whetten, Chem. Phys. Lett. 196 (1992) 330.
[23] Y. Tai, W. Yamaguchi, Y. Maruyama, K. Yoshimura, J. Murakami, J. Chem. Phys. 113 (2002) 3808.
[24] A. Terasaki, T. Tsukudas, H. Yasumatsu, T. Sugai, T. Kondow, J. Chem. Phys. 104 (1996) 1387.
[25] R. Beck, P.St. John, M.L. Homer, R.L. Whetten, Science 253 (1991) 879.
[26] A. Van Luming, J. Reuss, Int. J. Mass Spectrom. Ion Phys. 27 (1978) 197.
[27] C.E. Klots, J. Phys. C: Solid State Phys. 92 (1988) 5864.
[28] H. Vach, A.D. Martino, M. Benslimade, M. Chatelet, F. Pradere, J. Chem. Phys. 100 (1994) 8526, and references therein.
[29] C.L. Cleveland, U. Landman, Science 257 (1992) 355.
[30] H.P. Cheng, C.L. Cleveland, U. Landman, Science 260 (1993) 1304.
[31] T. Raz, R.D. Levine, J. Am. Chem. Soc. 116 (1994) 11167.
[32] I. Scheck, J. Jortner, T. Raz, R.D. Levine, Chem. Phys. Lett. 257 (1996) 273.
[33] W. Christen, U. Even, Eur. Phys. J. D 24 (2003) 283.
[34] S. Koizumi, H. Yasumatsu, S. Otani, T. Kondow, J. Phys. Chem. A 106 (2002) 267.
[35] C. Mair, Z. Herman, T. Fiegele, J.H. Futrell, T.D. Märk, Int. J. Mass Spectrom. 188 (1999) L1.
[36] C. Mair, T. Fiegele, F. Biasoli, Z. Herman, T.D. Märk, J. Chem. Phys. 111 (1999) 2770.
[37] C. Mair, Z. Herman, J. Fedor, M. Lezius, T.D. Märk, J. Chem. Phys. 118 (2003) 1479.
[38] P.M.St. John, R.D. Beck, R.L. Whetten, Phys. Rev. Lett. 69 (1992) 1497.
[39] W. Christen, U. Even, J. Phys. Chem. A 102 (1998) 9420;
W. Christen, U. Even, Eur. Phys. J. D 9 (1999) 29;
W. Christen, U. Even, Eur. Phys. J. D 16 (2001) 87.
[40] H. Yasumatsu, A. Terasaki, T. Kondow, Int. J. Mass Spectrom. Ion Process. 174 (1998) 297.
[41] C. Mair, M. Lezius, Z. Herman, T.D. Märk, J. Chem. Phys. 118 (2003) 7090.
[42] F. Biasioli, T. Fiegele, C. Mair, Z. Herman, O. Echt, F. Aumayr, H.P. Winter, T.D. Märk, J. Chem. Phys. 113 (2000) 5053.
[43] C. Mair, T. Fiegele, F. Biasioli, R. Worgotter, V. Grill, M. Lezius, T.D. Märk, Plasma Sources Sci. Technol. 8 (1999) 191.
[44] R.D. Beck, P.St. John, M.M. Alvarez, F. Diederich, R.L. Whetten, J. Phys. Chem. 95 (1991) 8402.
[45] H.G. Busman, T. Lill, I.V. Hertel, Chem. Phys. Lett. 187 (1991) 459.
[46] C. Yeretzian, R.L. Whetten, Z. Phys. D 24 (1992) 199.
[47] W. Forst, Theory of Unimolecular Reactions, Academic Press, New York, 1973.
[48] J.I. Brauman, in: P. Ausloos (Ed.), Kinetics of Ion–Molecule Reactions, Plenum Press, New York and London, 1979, p. 155.
[49] K.D. Cook, G.G. Jones, J.W. Taylor, Int. J. Mass Spectrom. Ion Phys. 35 (1980) 273.
[50] W.Y. Feng, M. Iraqui, C. Lifschtz, J. Phys. Chem. 97 (1993) 3510.
[51] D.S. Bomse, J.L. Beauchamp, J. Am. Chem. Soc. 103 (1981) 3292.
[52] J. Kubišta, Z. Dolejšek, Z. Herman, Eur. Mass Spectrom. 4 (1998) 311.
[53] J. Žabka, Z. Dolejšek, Z. Herman, J. Phys. Chem. A 106 (2002) 10861.
[54] V.M. Jarvis, M.A. Villanueva, D.E. Bostwick, T.D. Moran, Org. Mass Spectrom. 28 (1993) 595.
[55] S.A. Miller, D.E. Riederer, R.G. Cooks, W.R. Cho, H.W. Lee, H. Kang, J. Phys. Chem. 98 (1994) 245.